Available online at www.sciencedirect.com

ScienceDirect

Journal of Electrocardiology 49 (2016) 401 - 409

JOURNAL OF Electrocardiology

www.jecgonline.com

Heart morphology differences induced by intrauterine growth restriction and preterm birth measured on the ECG at preadolescent age

Nuria Ortigosa, Ph.D., [a,*] Merida Rodriguez-Lopez, MD, [b] Raquel Bailón, Ph.D., [c, d]
Sebastian Imre Sarvari, MD, Ph.D., [e, f] Marta Sitges, MD, Ph.D., [e]
Eduard Gratacos, MD, Ph.D., [b] Bart Bijnens, Ph.D, [g]
Fatima Crispi, MD, Ph.D., [b] Pablo Laguna, Ph.D. [c, d]

[a] *I.U. Matemática Pura y Aplicada, Universitat Politècnica de València Camino. de Vera s/n, 46022, Valencia, Spain*
[b] *Fetal i+D Medicine Research Center, BCNatal-Barcelona Center for Maternal-Fetal and Neonatal Medicine (Hospitals Clinic and Sant Joan de Deu). IDIBAPS, University of Barcelona (CIBER-ER)*
[c] *BSICoS Group, Aragón Institute of Engineering Research (I3A), IIS Aragón. University of Zaragoza, Spain*
[d] *Centro de Investigación Biomédica en Red en Bioingeniería, Biomateriales y Nanomedicina (CIBER-BBN), Spain*
[e] *Cardiovascular Institute, Hospital Clinic, IDIBAPS, University of Barcelona, Institut d'Investigacions Biomèdiques August Pi i Sunyer, Barcelona, Spain*
[f] *Department of Cardiology, Oslo University Hospital, Rikshospitalet, and University of Oslo, Norway*
[g] *ICREA, Universitat Pompeu Fabra, Spain*

Intrauterine Growth Restriction (IUGR) and premature birth are associated with higher risk of cardiovascular diseases throughout adulthood. The aim of this study was to evaluate the influence of these factors in ventricular electrical remodeling in preadolescents. Electrocardiography was performed in a cohort of 33-IUGR, 32-preterm with appropriate weight and 60 controls. Depolarization and repolarization processes were studied by means of the surface ECG, including loops and angles corresponding to QRS and T-waves. The angles between the dominant vector of QRS and the frontal plane XY were different among the study groups: controls [20.03°(10.11°-28.64°)], preterm [25.48°(19.79°-33.56°)], and IUGR [27.77°(16.59°-33.23°)]. When compared to controls, IUGR subjects also presented wider angles between the difference of QRS and T-wave dominant vectors and the XY-plane [5.28° ± 12.15° vs 0.49° ± 14.15°, p b 0.05] while preterm ones showed smaller frontal QRS-T angle [4.68°(2.20°-12.89°) vs 6.57°(2.72°-11.31°), p b 0.05]. Thus, electrical remodeling is present in IUGR and preterm preadolescents, and might predispose them to cardiovascular diseases in adulthood. Follow-up studies are warranted.

Keywords: Premature birth; Intrauterine Growth Restriction; ventricular electrical remodeling

1. Introduction

For many years, genetics and lifestyle have been considered as the main cardiovascular risk factors. However, by the 90s, Barker and colleagues demonstrated a strong association between cardiovascular diseases (CVD) and birthweight [1], and proposed that low birthweight may produce structural and functional changes in key organs in postnatal life that predispose to CVD in adulthood, from which the concept of fetal programming emerged [1]. In this paper, we studied two leading causes of low birthweight: intrauterine growth restriction (IUGR) and preterm delivery.

IUGR affects 7–10% of pregnancies and is defined as the failure of a fetus to achieve its growth potential [2]. It is usually associated with placental insufficiency that determines fetal hypoxia, undernutrition and pressure/volume overload. Several studies have demonstrated that IUGR fetuses [3] and children with earlier IUGR [4] show significant changes in cardiac structure and function in the form of more spherical hearts with reduced longitudinal motion and impaired relaxation. On the other hand, prematurity represents 4–10% of deliveries and is defined by birth before 37 completed weeks of gestation. Preterm birth has multiple causes, including spontaneous preterm labor, intraamniotic inflammation and/or infection, preterm rupture of membranes, and labor induction due to IUGR or preeclampsia. Recently, increased cardiac mass together with short and small left ventricles have been described in adults born preterm [5].

* Corresponding author.
E-mail address: nuorar@upvnet.upv.es

http://dx.doi.org/10.1016/j.jelectrocard.2016.03.011
0022-0736/

Available online at www.sciencedirect.com

ScienceDirect

Journal of Electrocardiology 49 (2016) 401 – 409

JOURNAL OF Electrocardiology

www.jecgonline.com

Heart morphology differences induced by intrauterine growth restriction and preterm birth measured on the ECG at preadolescent age

Nuria Ortigosa, Ph.D.,[a,*] Merida Rodriguez-Lopez, MD,[b] Raquel Bailón, Ph.D.,[c,d] Sebastian Imre Sarvari, MD, Ph.D.,[e,f] Marta Sitges, MD, Ph.D.,[e] Eduard Gratacos, MD, Ph.D.,[b] Bart Bijnens, Ph.D,[g] Fatima Crispi, MD, Ph.D.,[b] Pablo Laguna, Ph.D.[c,d]

[a] I.U. Matemática Pura y Aplicada, Universitat Politècnica de València Camino. de Vera s/n, 46022, Valencia, Spain
[b] Fetal i+D Medicine Research Center, BCNatal-Barcelona Center for Maternal-Fetal and Neonatal Medicine (Hospitals Clinic and Sant Joan de Deu). IDIBAPS, University of Barcelona (CIBER-ER)
[c] BSICoS Group, Aragón Institute of Engineering Research (I3A), IIS Aragón. University of Zaragoza, Spain
[d] Centro de Investigación Biomédica en Red en Bioingeniería, Biomateriales y Nanomedicina (CIBER-BBN), Spain
[e] Cardiovascular Institute, Hospital Clinic, IDIBAPS, University of Barcelona, Institut d'Investigacions Biomèdiques August Pi i Sunyer, Barcelona, Spain
[f] Department of Cardiology, Oslo University Hospital, Rikshospitalet, and University of Oslo, Norway
[g] ICREA, Universitat Pompeu Fabra, Spain

Intrauterine Growth Restriction (IUGR) and premature birth are associated with higher risk of cardiovascular diseases throughout adulthood. The aim of this study was to evaluate the influence of these factors in ventricular electrical remodeling in preadolescents. Electrocardiography was performed in a cohort of 33-IUGR, 32-preterm with appropriate weight and 60 controls. Depolarization and repolarization processes were studied by means of the surface ECG, including loops and angles corresponding to QRS and T-waves. The angles between the dominant vector of QRS and the frontal plane XY were different among the study groups: controls [20.03°(10.11°-28.64°)], preterm [25.48°(19.79°-33.56°)], and IUGR [27.77°(16.59°-33.23°)]. When compared to controls, IUGR subjects also presented wider angles between the difference of QRS and T-wave dominant vectors and the XY-plane [5.28° ± 12.15° vs 0.49° ± 14.15°, $p < 0.05$] while preterm ones showed smaller frontal QRS-T angle [4.68°(2.20°-12.89°) vs 6.57°(2.72°-11.31°), $p < 0.05$]. Thus, electrical remodeling is present in IUGR and preterm preadolescents, and might predispose them to cardiovascular diseases in adulthood. Follow-up studies are warranted.

Keywords: Premature birth; Intrauterine Growth Restriction; ventricular electrical remodeling

1. Introduction

For many years, genetics and lifestyle have been considered as the main cardiovascular risk factors. However, by the 90s, Barker and colleagues demonstrated a strong association between cardiovascular diseases (CVD) and birthweight [1], and proposed that low birthweight may produce structural and functional changes in key organs in postnatal life that predispose to CVD in adulthood, from which the concept of fetal programming emerged [1]. In this paper, we studied two leading causes of low birthweight: intrauterine growth restriction (IUGR) and preterm delivery.

IUGR affects 7–10% of pregnancies and is defined as the failure of a fetus to achieve its growth potential [2]. It is usually associated with placental insufficiency that determines fetal hypoxia, undernutrition and pressure/volume overload. Several studies have demonstrated that IUGR fetuses [3] and children with earlier IUGR [4] show significant changes in cardiac structure and function in the form of more spherical hearts with reduced longitudinal motion and impaired relaxation. On the other hand, prematurity represents 4–10% of deliveries and is defined by birth before 37 completed weeks of gestation. Preterm birth has multiple causes, including spontaneous preterm labor, intraamniotic inflammation and/or infection, preterm rupture of membranes, and labor induction due to IUGR or preeclampsia. Recently, increased cardiac mass together with short and small left ventricles have been described in adults born preterm [5].

* Corresponding author.
E-mail address: nuorar@upvnet.upv.es

http://dx.doi.org/10.1016/j.jelectrocard.2016.03.011
0022-0736/

In addition, both IUGR and prematurity have been associated with increased CVD in adulthood [6] as well as with arrhythmias, i.e. sudden death syndrome [7] and apnea-bradycardia episodes [8] in infants. However, little is known about the presence of electrical changes associated with these conditions that could predispose to long-term consequences. It has been proposed that electrical remodeling could occur primarily or secondary to the cardiac structural remodeling described in these conditions [9].

Hence, the aim of the present study was to identify signs of ventricular electrical remodeling in preterm and growth restricted babies on reaching preadolescence by assessing changes in ventricular depolarization and repolarization using the QRS complex and T-wave, respectively. This was assessed by analyzing the direction of the QRS and T vectors, as well as the angle between them, which is supposed to reflect possible deviations between ventricular depolarization and repolarization. Finally, an analysis of QRS and T loop morphology was also performed in order to study in detail the presence of abnormalities in the ECG signal.

2. Materials and methods

2.1. Study populations

The study population included 125 preadolescents, whose surface 12-lead ECG was recorded at a sampling rate of 1000 Hz in a tertiary center. 33 subjects had severe IUGR with medically-induced preterm delivery, 32 were spontaneously born preterm with appropriate weight for gestational age (AGA) and 60 normally grown controls born at term. From now on, these three groups will be denoted by preterm-IUGR, preterm-AGA and controls. IUGR was defined by low birthweight below 10th centile and abnormal umbilical artery Doppler (pulsatility index above the 95th centile), while adequate growth was considered if birthweight was above 10th centile for gestational age according to local standards [10]. Preterm birth was defined by delivery before 37 completed weeks of gestation. Gestational age was calculated by first-trimester crown-rump length measurement by ultrasound. Cases and controls were selected from a previously published cohort study that included 200 children at 2–6 years of age whose gestational age ranged from 25 to 41 weeks [4], which was conducted in a tertiary referral university hospital in Barcelona, Spain. We contacted all previous study participants to be included in this follow-up (6 years after the previous cardiovascular assessment) and 125 accepted to be recruited for the present study.

Digital standard 12-lead surface ECGs were recorded using a Gem Heart One recorder (Gem-Med SL, Spain), at an equivalent paper speed of 50 mm/s and a gain of 10 mm/mV. This recorder provided digital recordings in SCP format. The acquisition process was performed by a trained nurse.

2.2. Signal preprocessing

ECG was delineated so that QRS complexes and T waves, as well as their onset and end, were detected. This was performed by a wavelet transform delineation technique [11]. Then, baseline wander was reduced by means of cubic splines [12]. The vectorcardiogram was synthesized using the inverse Dower matrix [13].

2.3. Loop alignment and averaging

In order to attenuate noise, respiratory influence and muscular activity, depolarization and repolarization loops were first aligned with respect to a reference loop and then averaged. The reference loop is selected as the first visually checked normal loop, Z_R, consisting of a $3 \times (k + 2\Delta)$ matrix containing at each row the leads X, Y and Z, respectively. Spatial and temporal alignment was performed in terms of scaling, rotation and time synchronization of the loops, as presented in [14].

Thus, three transformations were considered to perform the alignment. This process can be described as:

$$Z \approx \alpha R Z_R J_\tau \qquad (1)$$

where Z and Z_R denote the $3 \times K$ and $3 \times (K + 2\Delta)$ matrices that contain in each row K or $K + 2\Delta$ samples corresponding to leads X, Y, Z of the loop to be aligned and the reference loop, respectively. Scaling was controlled by the positive parameter α, that allows loop expansion or contraction, whereas rotational changes of the heart were introduced by the 3×3 rotation matrix R. Finally, time synchronization was described by the integer time shift τ in the shift matrix J_τ, which was defined as

$$J_\tau \approx \begin{bmatrix} 0_{\Delta+\tau} \\ I \\ 0_{\Delta-\tau} \end{bmatrix}$$

where $\tau = -\Delta, \ldots, \Delta$, the identity matrix I is $K \times K$, and the top and bottom zero matrices are $(\Delta + \tau) \times K$ and $(\Delta - \tau) \times K$, respectively. Parameter Δ corresponds to the 2Δ additional samples that the reference loop Z_R has in order to allow for time synchronization of observations of different subsets of K samples.

The optimal estimates for α, τ and R were determined by solving the minimization problem

$$\varepsilon^2_{min} \approx \min_{\alpha, R, \tau} \left\| Z - \alpha R Z_R J_\tau \right\|^2_F \qquad (2)$$

where ε^2 represents the error, calculated as the Frobenius norm of the difference between the actual and the reference loop subjected to the transformations. ε^2 is minimized by first finding the estimates for α and R for every value of τ and then selecting the value of τ that minimizes the error. For a fully detailed explanation of the alignment process see [14].

Depolarization loops are aligned and the estimated transformations for each heartbeat are applied to align the repolarization loops. Then, depolarization and repolarization loops are averaged in order to obtain a clean and robust mean QRS and T loop. Then, the dominant vectors of the average loops, denoted by v_{QRS} and v_T, are obtained by averaging the whole set of vectors that form each loop. These set of vectors describe the dominant direction of the electrical

In addition, both IUGR and prematurity have been associated with increased CVD in adulthood [6] as well as with arrhythmias, i.e. sudden death syndrome [7] and apnea-bradycardia episodes [8] in infants. However, little is known about the presence of electrical changes associated with these conditions that could predispose to long-term consequences. It has been proposed that electrical remodeling could occur primarily or secondary to the cardiac structural remodeling described in these conditions [9].

Hence, the aim of the present study was to identify signs of ventricular electrical remodeling in preterm and growth restricted babies on reaching preadolescence by assessing changes in ventricular depolarization and repolarization using the QRS complex and T-wave, respectively. This was assessed by analyzing the direction of the QRS and T vectors, as well as the angle between them, which is supposed to reflect possible deviations between ventricular depolarization and repolarization. Finally, an analysis of QRS and T loop morphology was also performed in order to study in detail the presence of abnormalities in the ECG signal.

2. Materials and methods

2.1. Study populations

The study population included 125 preadolescents, whose surface 12-lead ECG was recorded at a sampling rate of 1000 Hz in a tertiary center. 33 subjects had severe IUGR with medically-induced preterm delivery, 32 were spontaneously born preterm with appropriate weight for gestational age (AGA) and 60 normally grown controls born at term. From now on, these three groups will be denoted by preterm-IUGR, preterm-AGA and controls. IUGR was defined by low birthweight below 10th centile and abnormal umbilical artery Doppler (pulsatility index above the 95th centile), while adequate growth was considered if birthweight was above 10th centile for gestational age according to local standards [10]. Preterm birth was defined by delivery before 37 completed weeks of gestation. Gestational age was calculated by first-trimester crown-rump length measurement by ultrasound. Cases and controls were selected from a previously published cohort study that included 200 children at 2–6 years of age whose gestational age ranged from 25 to 41 weeks [4], which was conducted in a tertiary referral university hospital in Barcelona, Spain. We contacted all previous study participants to be included in this follow-up (6 years after the previous cardiovascular assessment) and 125 accepted to be recruited for the present study.

Digital standard 12-lead surface ECGs were recorded using a Gem Heart One recorder (Gem-Med SL, Spain), at an equivalent paper speed of 50 mm/s and a gain of 10 mm/mV. This recorder provided digital recordings in SCP format. The acquisition process was performed by a trained nurse.

2.2. Signal preprocessing

ECG was delineated so that QRS complexes and T waves, as well as their onset and end, were detected. This was performed by a wavelet transform delineation technique [11]. Then, baseline wander was reduced by means of cubic splines [12]. The vectorcardiogram was synthesized using the inverse Dower matrix [13].

2.3. Loop alignment and averaging

In order to attenuate noise, respiratory influence and muscular activity, depolarization and repolarization loops were first aligned with respect to a reference loop and then averaged. The reference loop is selected as the first visually checked normal loop, $\mathbf{Z_R}$, consisting of a $3\times(k+2\Delta)$ matrix containing at each row the leads X, Y and Z, respectively. Spatial and temporal alignment was performed in terms of scaling, rotation and time synchronization of the loops, as presented in [14].

Thus, three transformations were considered to perform the alignment. This process can be described as:

$$\mathbf{Z} = \alpha \mathcal{Q} \mathbf{Z_R} \mathbf{J}_\tau \tag{1}$$

where $\mathbf{Z}$ and $\mathbf{Z_R}$ denote the $3 \times K$ and $3 \times (\mathrm{K} + 2\,\Delta)$ matrices that contain in each row K or $\mathrm{K} + 2\,\Delta$ samples corresponding to leads X,Y,Z of the loop to be aligned and the reference loop, respectively. Scaling was controlled by the positive parameter α, that allows loop expansion or contraction, whereas rotational changes of the heart were introduced by the 3×3 rotation matrix $\mathcal{Q}$. Finally, time synchronization was described by the integer time shift τ in the shift matrix $\mathbf{J}_\tau$, which was defined as

$$\mathbf{J}_\tau = \begin{bmatrix} 0_{\Delta+\tau} \\ I \\ 0_{\Delta-\tau} \end{bmatrix}$$

where $\tau = -\Delta, \ldots, \Delta$, the identity matrix I is $K\times K$, and the top and bottom zero matrices are $(\Delta+\tau)\times K$ and $(\Delta-\tau)\times K$, respectively. Parameter Δ corresponds to the 2Δ additional samples that the reference loop $\mathbf{Z_R}$ has in order to allow for time synchronization of observations of different subsets of K samples.

The optimal estimates for α, τ and $\mathcal{Q}$ were determined by solving the minimization problem

$$\epsilon^2_{min} = \min_{\alpha,\mathcal{Q},\tau} \left\| \mathbf{Z} - \alpha \mathcal{Q} \mathbf{Z_R} \mathbf{J}_\tau \right\|^2_F \tag{2}$$

where ε^2 represents the error, calculated as the Frobenius norm of the difference between the actual and the reference loop subjected to the transformations. ε^2 is minimized by first finding the estimates for α and $\mathcal{Q}$ for every value of τ and then selecting the value of τ that minimizes the error. For a fully detailed explanation of the alignment process see [14].

Depolarization loops are aligned and the estimated transformations for each heartbeat are applied to align the repolarization loops. Then, depolarization and repolarization loops are averaged in order to obtain a clean and robust mean QRS and T loop. Then, the dominant vectors of the average loops, denoted by $\mathbf{v}_{QRS}$ and $\mathbf{v}_T$, are obtained by averaging the whole set of vectors that form each loop. These set of vectors describe the dominant direction of the electrical

wavefront along the depolarization (v_{QRS}) and the repolarization (v_T) processes.

2.4. Angles estimation based on dominant vectors of depolarization and repolarization loops

We estimated the angle between the dominant vectors of depolarization and repolarization phases in the three dimensional space (θ_{RT}, the so-called spatial QRS-T angle). It is defined as the angle measured in the plane that formed by the maximum vectors of the QRS complex and the T-wave. It usually differs from the angle of the projections of the QRS and T axes in the frontal plane XY, denoted by $\theta_{RT\text{-}XY}$, and which was also calculated in our study.

Next, we estimated the absolute angles between vectors v_{QRS} and v_T and the three orthogonal planes, Φ_{R-P} and Φ_{T-P}, where $P \in \{XZ, XY, YZ\}$ denotes each orthogonal plane formed by the two directions referred to P. Finally, we also estimated the difference between them with respect to each orthogonal plane.

2.5. Loop morphology

Loop morphology was assessed by means of planarity and roundness measurements. *Planarity* is a measure of how well the VCG can be approximated by a plane or whether it is not possible, since the VCG is so curved that it is really distributed along the 3D spatial loop. *Roundness* measurements were referred to 2D planar projections of the VCG, taking values in the range [0–1] (where 1 means that the projection is closer to a circle than to a straight line, whereas roundness close to 0 reflects the opposite and intermediate situations - an ellipsoidal shape of the VCG-) with different axes ratios as function of roundness.

If we denote the eigenvalues of the average loop matrix as λ_i, $i = 1, 2, 3$, sorted in descending order, the planarity of the loops is defined as

$$\rho_L = \frac{\lambda_3}{\lambda_1} \quad (3)$$

where ρ can take values between zero (entirely planar loop) and one (loop that equally extends into the three dimensions). Features will be obtained for both the depolarization and repolarization loops, being indicated by the subscript $_L$ values $_R$ or $_T$, respectively. Planarity can also be analyzed by features σ_L and δ_L, which can take values in the range [0–1] (reflecting more planar loops when σ_L is close to 1 and δ is close to 0):

$$r_L = \frac{\lambda_1 + \lambda_2}{\lambda_1 + \lambda_2 + \lambda_3} \quad (4)$$

$$d_L = \frac{\lambda_3}{\lambda_1 + \lambda_2} \quad (5)$$

QRS and T wave complexity was defined as the ratio between the second to the first eigenvalues, denoted by *C*:

$$C_L = \frac{\lambda_2}{\lambda_1} \quad (6)$$

The geometrical interpretation of *C* refers to the roundness of the loop [15]. This feature was also obtained for each plane $P \in \{XZ, XY, YZ\}$, corresponding to the loop projection onto each orthogonal plane. Eigenvalues obtained on the projection were v_1, v_2, sorted in descending order. Thus, the roundness of the loops projected on each plane was defined as

$$\varrho_{L-P} = \frac{m_2}{m_1} \quad (7)$$

2.6. Statistical analysis

A descriptive analysis including angles, planarity and characteristics was performed using mean ± standard deviation or median (interquartile range) to assess the differences between each group (Preterm-AGA and Preterm-IUGR) and controls. The results were compared by t-test or Wilcoxon-Mann–Whitney to compare means and standard deviations or medians and interquartile ranges, respectively, and χ^2 to compare percentages. Multivariate analysis by linear or quantile regression was used to adjust for age, height, gender and heart rate.

Table 1
Baseline and perinatal characteristics of the study populations. AGA (appropriate growth for gestational age), IUGR (intrauterine growth restriction). Data are mean ± standard deviation or median (interquartile range).

	Controls n = 60	Preterm AGA n = 32	Preterm IUGR n = 33
Birthweight (g)	3444 ± 379.4	1872 ± 614.7*	1162 ± 351.9*
Gestational age at delivery (weeks)	39.5 ± 1.3	31.6 ± 3.1*	32.0 ± 2.4*
Birthweight centile	56(37–81)	48(30–85)	0(0–0)*
Caucasian ethnicity (%)	95.1	93.9	80.0*
Male gender (%)	53.2	39.4	37.1
Age (years)	12.1(10.5–12.4)	10.4(8.5–11.3)*	9.41(8.3–11.4)*
Heart rate (bpm)	77.66 ± 11.83	88.30 ± 10.94*	81.4 ± 9.26*
Height (cm)	148.5(137.8–154.3)	135.2(129.7–145.1)*	135(129.2–147.5)*
Weight (kg)	43.3(35.9–48.0)	32.8(28.2–41.1)*	34.4 (28.5–41.7)*
Body mass index (kg/m^2)	19.0(17.1–20.6)	17.24(15.9–20.1)	18.1(16.4–19.6)

* $p < 0.05$ by t-test, Wilcoxon-Mann–Whitney or χ^2 as compared to controls.

wavefront along the depolarization ($\mathbf{v}_{QRS}$) and the repolarization ($\mathbf{v}_T$) processes.

2.4. Angles estimation based on dominant vectors of depolarization and repolarization loops

We estimated the angle between the dominant vectors of depolarization and repolarization phases in the three dimensional space (θ_{RT}, the so-called spatial QRS-T angle). It is defined as the angle measured in the plane that formed by the maximum vectors of the QRS complex and the T-wave. It usually differs from the angle of the projections of the QRS and T axes in the frontal plane XY, denoted by $\theta_{RT\text{-}XY}$, and which was also calculated in our study.

Next, we estimated the absolute angles between vectors $\mathbf{v}_{QRS}$ and $\mathbf{v}_T$ and the three orthogonal planes, $\Phi_{R-\mathcal{P}}$ and $\Phi_{T-\mathcal{P}}$, where $\mathcal{P}\in\{XZ, XY, YZ\}$ denotes each orthogonal plane formed by the two directions referred to $\mathcal{P}$. Finally, we also estimated the difference between them with respect to each orthogonal plane.

2.5. Loop morphology

Loop morphology was assessed by means of planarity and roundness measurements. *Planarity* is a measure of how well the VCG can be approximated by a plane or whether it is not possible, since the VCG is so curved that it is really distributed along the 3D spatial loop. *Roundness* measurements were referred to 2D planar projections of the VCG, taking values in the range [0–1] (where 1 means that the projection is closer to a circle than to a straight line, whereas roundness close to 0 reflects the opposite and intermediate situations - an ellipsoidal shape of the VCG-) with different axes ratios as function of roundness.

If we denote the eigenvalues of the average loop matrix as $\lambda_i, i=1,2,3$, sorted in descending order, the planarity of the loops is defined as

$$\rho_L = \frac{\lambda_3}{\lambda_1} \tag{3}$$

where ρ can take values between zero (entirely planar loop) and one (loop that equally extends into the three dimensions). Features will be obtained for both the depolarization and repolarization loops, being indicated by the subscript $_L$ values $_R$ or $_T$, respectively. Planarity can also be analyzed by features σ_L and δ_L, which can take values in the range [0–1] (reflecting more planar loops when σ_L is close to 1 and δ is close to 0):

$$\sigma_L = \frac{\lambda_1 + \lambda_2}{\lambda_1 + \lambda_2 + \lambda_3} \tag{4}$$

$$\delta_L = \frac{\lambda_3}{\lambda_1 + \lambda_2} \tag{5}$$

QRS and T wave complexity was defined as the ratio between the second to the first eigenvalues, denoted by C:

$$C_L = \frac{\lambda_2}{\lambda_1} \tag{6}$$

The geometrical interpretation of C refers to the roundness of the loop [15]. This feature was also obtained for each plane $\mathcal{P}\in\{XZ, XY, YZ\}$, corresponding to the loop projection onto each orthogonal plane. Eigenvalues obtained on the projection were v_1, v_2, sorted in descending order. Thus, the roundness of the loops projected on each plane was defined as

$$\varrho_{L-\mathcal{P}} = \frac{v_2}{v_1} \tag{7}$$

2.6. Statistical analysis

A descriptive analysis including angles, planarity and characteristics was performed using mean ± standard deviation or median (interquartile range) to assess the differences between each group (Preterm-AGA and Preterm-IUGR) and controls. The results were compared by t-test or Wilcoxon-Mann–Whitney to compare means and standard deviations or medians and interquartile ranges, respectively, and χ^2 to compare percentages. Multivariate analysis by linear or quantile regression was used to adjust for age, height, gender and heart rate.

Table 1
Baseline and perinatal characteristics of the study populations. AGA (appropriate growth for gestational age), IUGR (intrauterine growth restriction). Data are mean ± standard deviation or median (interquartile range).

	Controls n = 60	Preterm AGA n = 32	Preterm IUGR n = 33
Birthweight (g)	3444 ± 379.4	1872 ± 614.7*	1162 ± 351.9*
Gestational age at delivery (weeks)	39.5 ± 1.3	31.6 ± 3.1*	32.0 ± 2.4*
Birthweight centile	56(37–81)	48(30–85)	0(0–0)*
Caucasian ethnicity (%)	95.1	93.9	80.0*
Male gender (%)	53.2	39.4	37.1
Age (years)	12.1(10.5–12.4)	10.4(8.5–11.3)*	9.41(8.3–11.4)*
Heart rate (bpm)	77.66 ± 11.83	88.30 ± 10.94*	81.4 ± 9.26*
Height (cm)	148.5(137.8–154.3)	135.2(129.7–145.1)*	135(129.2–147.5)*
Weight (kg)	43.3(35.9–48.0)	32.8(28.2–41.1)*	34.4 (28.5–41.7)*
Body mass index (kg/m^2)	19.0(17.1–20.6)	17.24(15.9–20.1)	18.1(16.4–19.6)

* $p < 0.05$ by t-test, Wilcoxon-Mann–Whitney or χ^2 as compared to controls.

Table 2
Vectocardiographic angle features of the study population. θ_{RT} and $\theta_{RT\text{-}XY}$ denote the so-called spatial QRS-T and frontal QRS-T angles, respectively. Absolute angles between vectors $\mathbf{v}_{QRS}$ or $\mathbf{v}_{T}$ and the three orthogonal planes of the space are denoted by $\Phi_{R\text{-}\mathcal{P}}$ and $\Phi_{T\text{-}\mathcal{P}}$, where $\mathcal{P} \in \{XZ, XY, YZ\}$ refers to each orthogonal plane. AGA (appropriate growth for gestational age), IUGR (intrauterine growth restriction). Subscripts R and T refer to the depolarization and repolarization loops, respectively. Data are mean ± standard deviation or median (interquartile range).

	Controls n = 60	Preterm AGA n = 32	Preterm IUGR n = 33
θ_{RT}	15.28(8.390–24.10)	10.63(5.539–20.76)	16.58(6.890–22.73)
θ_{RT-XY}	6.57(2.72–11.31)	4.68(2.20–12.89)†	6.52(3.88–15.82)
Φ_{R-XZ}	37.60(29.91–40.82)	32.64(28.90–36.78)*	34.24(28.58–39.91)
Φ_{R-XY}	20.03(10.11–28.64)	27.77(16.59–33.23)*	25.48(19.79–33.56)*†
Φ_{R-YZ}	45.95 ± 9.31	45.85 ± 9.02	43.06 ± 8.92
Φ_{T-XZ}	36.42(32.05–38.83)	31.89(29.07–38.14)	32.01(28.58–38.63)†
Φ_{T-XY}	29.39(13.71–27.26)	23.59(17.63–26.80)	21.52(12.77–25.89)
Φ_{T-YZ}	47.24(38.75–52.86)	46.57(41.63–53.30)	47.86(41.16–56.55)
$\Phi_{R-XZ} - \Phi_{T-XZ}$	1.70(−3.97–5.43)	−0.52(−6.01–4.69)	0.88(2.33–6.10)
$\Phi_{R-XY} - \Phi_{T-XY}$	−0.491 ± 14.15	3.001 ± 12.99	5.279 ± 12.15*†
$\Phi_{R-YZ} - \Phi_{T-YZ}$	−0.662 ± 12.50	−1.752 ± 10.67	−4.854 ± 12.74

* p-value b 0.05 by Wilcoxon-Mann–Whitney or t-test as compared to controls. † p-value b 0.05 adjusted by age, height, gender and heart rate, controls as reference category.

3. Results

Estimated angles and morphology measurements were obtained on the cohort of 125 subjects described in Section 2.1, who form the three groups under study: 60 controls, 32 preterm-AGA, 33 preterm-IUGR. The median and interquartile ranges of the explored parameters are shown in Tables 2 and 3, whereas perinatal and anthropometric characteristics of the study populations are shown in Table 1.

As expected, both preterm-IUGR and preterm-AGA cases presented lower birthweight and gestational age at delivery as compared with controls. Preterm-IUGR cases also showed a lower birthweight centile as compared with controls and preterm-AGA. The proportion of males was similar among groups, while the preterm-IUGR subgroup presented a lower prevalence of Caucasian ethnicity. Heart rate was significatively higher for preterm-AGA and preterm-IUGR, since these subjects had lower stroke volume which was compensated by increasing the heart rate [4]. Both preterm-IUGR and preterm-AGA cases showed significantly lower age, height and weight (with preserved body mass index) at evaluation as compared with controls. All subjects were asymptomatic, and none of them received medication for any cardiac condition.

Tables 2 and 3 also highlight obtained p-values lower than 0.05 by applying the Wilcoxon-Mann-Witney or the Student's t-test for the comparisons between the three different groups of subjects. We studied differences between the control group and the preterm-AGA and preterm-IUGR groups.

Fig. 1 depicts the graphical comparison between the three groups (one example of each group under study, in pairs). In this Figure, a comparison of the preterm-AGA and the preterm-IUGR groups with respect to the control group was

Table 3
Vectocardiographic loops morphology of the study population. ρ_{L}, σ_{L}, and δ_{L} denote measures of planarity of loop L. C_{L} and $\varrho_{L\text{-}\mathcal{P}}$ refer to roundness measurements. $\mathcal{P} \in \{XZ, XY, YZ\}$ refers to the projection of the loop in each orthogonal plane $\mathcal{P}$, whereas the subscript L will be replaced by R or T, depending on whether it refers to the depolarization or repolarization loops. AGA (appropriate growth for gestational age), IUGR (intrauterine growth restriction). Subscripts R and T refer to the depolarization and repolarization loops, respectively. Data are median (interquartile range).

	Controls n = 60	Preterm AGA n = 32	Preterm IUGR n = 33
ρ_{R}	0.044(0.029–0.067)	0.036(0.022–0.058)	0.037(0.022–0.051)
ρ_{T}	0.031(0.021–0.054)	0.037(0.028–0.061)	0.034(0.021–0.048)
σ_{R}	0.967(0.953–0.979)	0.975(0.956–0.982)	0.971(0.961–0.982)
σ_{T}	0.973(0.955–0.981)	0.968(0.946–0.976)	0.972(0.955–0.981)
δ_{R}	0.033(0.022–0.045)	0.024(0.017–0.046)	0.028(0.017–0.040)
δ_{T}	0.028(0.019–0.044)	0.031(0.024–0.054)	0.027(0.019–0.044)
C_{R}	0.316(0.222–0.423)	0.264(0.171–0.331)	0.291(0.202–0.420)
C_{T}	0.135(0.103–0.189)	0.149(0.123–0.192)	0.134(0.096–0.189)
ϱ_{R-XZ}	0.384(0.257–0.489)	0.291(0.194–0.396)*†	0.335(0.247–0.516)
ϱ_{R-XY}	0.113(0.066–0.162)	0.086(0.049–0.155)†	0.117(0.074–0.187)
ϱ_{R-YZ}	0.330(0.211–0.452)	0.227(0.164–0.331)*†	0.276(0.212–0.346)
ϱ_{T-XZ}	0.157(0.124–0.198)	0.166(0.113–0.204)	0.141(0.102–0.235)
ϱ_{T-XY}	0.054(0.037–0.067)	0.072(0.042–0.110)*	0.054(0.032–0.095)
ϱ_{T-YZ}	0.201(0.151–0.272)	0.155(0.111–0.235)*	0.171(0.134–0.281)

* p-value b 0.05 by Wilcoxon-Mann–Whitney or t-test as compared to controls. † p-value b 0.05 adjusted by age, height, gender and heart rate, controls as reference category.

Table 2
Vectocardiographic angle features of the study population. θ_{RT} and $\theta_{RT\text{-}XY}$ denote the so-called spatial QRS-T and frontal QRS-T angles, respectively. Absolute angles between vectors $\mathbf{v}_{QRS}$ or $\mathbf{v}_{T}$ and the three orthogonal planes of the space are denoted by $\Phi_{R-\mathcal{P}}$ and $\Phi_{T-\mathcal{P}}$, where $\mathcal{P} \in \{XZ, XY, YZ\}$ refers to each orthogonal plane. AGA (appropriate growth for gestational age), IUGR (intrauterine growth restriction). Subscripts R and T refer to the depolarization and repolarization loops, respectively. Data are mean ± standard deviation or median (interquartile range).

	Controls n = 60	Preterm AGA n = 32	Preterm IUGR n = 33
θ_{RT}	15.28(8.390–24.10)	10.63(5.539–20.76)	16.58(6.890–22.73)
θ_{RT-XY}	6.57(2.72–11.31)	4.68(2.20–12.89)†	6.52(3.88–15.82)
Φ_{R-XZ}	37.60(29.91–40.82)	32.64(28.90–36.78)*	34.24(28.58–39.91)
Φ_{R-XY}	20.03(10.11–28.64)	27.77(16.59–33.23)*	25.48(19.79–33.56)*†
Φ_{R-YZ}	45.95 ± 9.31	45.85 ± 9.02	43.06 ± 8.92
Φ_{T-XZ}	36.42(32.05–38.83)	31.89(29.07–38.14)	32.01(28.58–38.63)†
Φ_{T-XY}	29.39(13.71–27.26)	23.59(17.63–26.80)	21.52(12.77–25.89)
Φ_{T-YZ}	47.24(38.75–52.86)	46.57(41.63–53.30)	47.86(41.16–56.55)
$\Phi_{R-XZ} - \Phi_{T-XZ}$	1.70(−3.97–5.43)	−0.52(−6.01–4.69)	0.88(2.33–6.10)
$\Phi_{R-XY} - \Phi_{T-XY}$	−0.491 ± 14.15	3.001 ± 12.99	5.279 ± 12.15*†
$\Phi_{R-YZ} - \Phi_{T-YZ}$	−0.662 ± 12.50	−1.752 ± 10.67	−4.854 ± 12.74

* p-value < 0.05 by Wilcoxon-Mann–Whitney or t-test as compared to controls. † p-value < 0.05 adjusted by age, height, gender and heart rate, controls as reference category.

3. Results

Estimated angles and morphology measurements were obtained on the cohort of 125 subjects described in Section 2.1, who form the three groups under study: 60 controls, 32 preterm-AGA, 33 preterm-IUGR. The median and interquartile ranges of the explored parameters are shown in Tables 2 and 3, whereas perinatal and anthropometric characteristics of the study populations are shown in Table 1.

As expected, both preterm-IUGR and preterm-AGA cases presented lower birthweight and gestational age at delivery as compared with controls. Preterm-IUGR cases also showed a lower birthweight centile as compared with controls and preterm-AGA. The proportion of males was similar among groups, while the preterm-IUGR subgroup presented a lower prevalence of Caucasian ethnicity. Heart rate was significatively higher for preterm-AGA and preterm-IUGR, since these subjects had lower stroke volume which was compensated by increasing the heart rate [4]. Both preterm-IUGR and preterm-AGA cases showed significantly lower age, height and weight (with preserved body mass index) at evaluation as compared with controls. All subjects were asymptomatic, and none of them received medication for any cardiac condition.

Tables 2 and 3 also highlight obtained p-values lower than 0.05 by applying the Wilcoxon-Mann-Witney or the Student's t-test for the comparisons between the three different groups of subjects. We studied differences between the control group and the preterm-AGA and preterm-IUGR groups.

Fig. 1 depicts the graphical comparison between the three groups (one example of each group under study, in pairs). In this Figure, a comparison of the preterm-AGA and the preterm-IUGR groups with respect to the control group was

Table 3
Vectocardiographic loops morphology of the study population. ρ_{L}, σ_{L}, and δ_{L} denote measures of planarity of loop L. C_{L} and $\varrho_{L-\mathcal{P}}$ refer to roundness measurements. $\mathcal{P} \in \{XZ, XY, YZ\}$ refers to the projection of the loop in each orthogonal plane $\mathcal{P}$, whereas the subscript L will be replaced by R or T, depending on whether it refers to the depolarization or repolarization loops. AGA (appropriate growth for gestational age), IUGR (intrauterine growth restriction). Subscripts R and T refer to the depolarization and repolarization loops, respectively. Data are median (interquartile range).

	Controls n = 60	Preterm AGA n = 32	Preterm IUGR n = 33
ρ_{R}	0.044(0.029–0.067)	0.036(0.022–0.058)	0.037(0.022–0.051)
ρ_{T}	0.031(0.021–0.054)	0.037(0.028–0.061)	0.034(0.021–0.048)
σ_{R}	0.967(0.953–0.979)	0.975(0.956–0.982)	0.971(0.961–0.982)
σ_{T}	0.973(0.955–0.981)	0.968(0.946–0.976)	0.972(0.955–0.981)
δ_{R}	0.033(0.022–0.045)	0.024(0.017–0.046)	0.028(0.017–0.040)
δ_{T}	0.028(0.019–0.044)	0.031(0.024–0.054)	0.027(0.019–0.044)
C_{R}	0.316(0.222–0.423)	0.264(0.171–0.331)	0.291(0.202–0.420)
C_{T}	0.135(0.103–0.189)	0.149(0.123–0.192)	0.134(0.096–0.189)
ϱ_{R-XZ}	0.384(0.257–0.489)	0.291(0.194–0.396)*†	0.335(0.247–0.516)
ϱ_{R-XY}	0.113(0.066–0.162)	0.086(0.049–0.155)†	0.117(0.074–0.187)
ϱ_{R-YZ}	0.330(0.211–0.452)	0.227(0.164–0.331)*†	0.276(0.212–0.346)
ϱ_{T-XZ}	0.157(0.124–0.198)	0.166(0.113–0.204)	0.141(0.102–0.235)
ϱ_{T-XY}	0.054(0.037–0.067)	0.072(0.042–0.110)*	0.054(0.032–0.095)
ϱ_{T-YZ}	0.201(0.151–0.272)	0.155(0.111–0.235)*	0.171(0.134–0.281)

* p-value <0.05 by Wilcoxon-Mann–Whitney or t-test as compared to controls. † p-value <0.05 adjusted by age, height, gender and heart rate, controls as reference category.

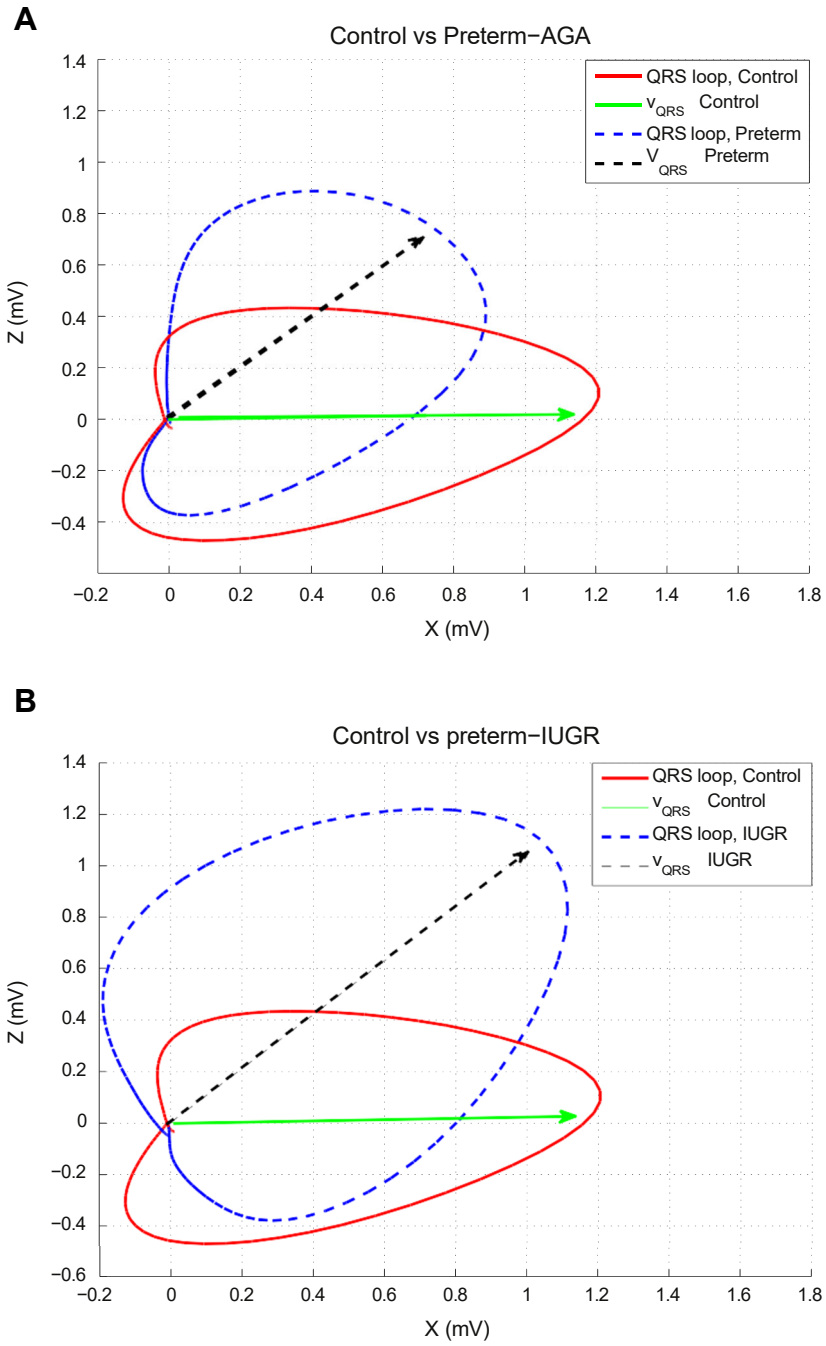

Fig. 1. Average of all depolarization loops for a patient and their corresponding dominant vectors ($\mathbf{v}_{QRS}$) projected onto the XZ-plane. (A) Subject of the control group vs. a subject from the preterm group. (B) Same subject of the control group vs. a subject from the IUGR group.

represented, whereas Fig. 2 shows the comparison between the dominant vectors of the depolarization and repolarization loops for the analysis of one subject from the preterm-IUGR and another subject from the preterm-AGA. Furthermore, for the sake of clarity in graphical representation, the projections of the loops on the plane with clearer differences were represented (instead of representing them in the three-dimensional space).

In general, preterm-AGA and preterm-IUGR subjects presented larger values for angle measurement $\Phi_{R\text{-}XY}$ than controls, being also statistically significant when adjusting the data by age, height, gender and heart rate. In the particular case of preterm-IUGR, the angle difference $\Phi_{R\text{-}XY} - \Phi_{T\text{-}XY}$ was also significant, being even larger than for the preterm-AGA group. Roundness measurements revealed significant differences between preterm-AGA and control groups, presenting the latter ones lower roundness measurements when analyzing the depolarization loops in the planes XZ and YZ.

4. Discussion of results

This paper reports for the first time significant changes in depolarization-repolarization angles and VCG loop morphology in IUGR and preterm individuals, respectively. These findings support the notion of electrophysiological remodeling in both IUGR and prematurity, and could

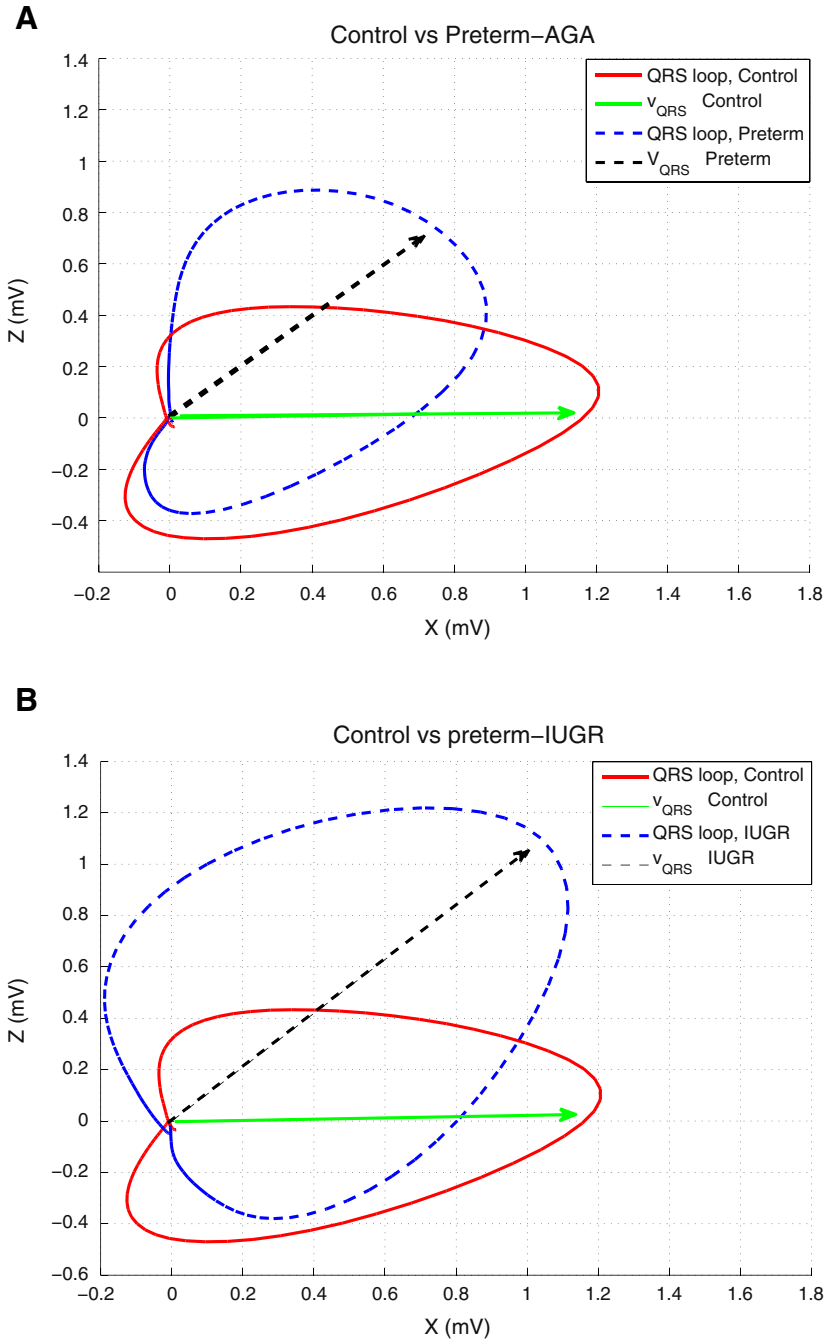

Fig. 1. Average of all depolarization loops for a patient and their corresponding dominant vectors ($\boldsymbol{v}_{QRS}$) projected onto the XZ-plane. (A) Subject of the control group vs. a subject from the preterm group. (B) Same subject of the control group vs. a subject from the IUGR group.

represented, whereas Fig. 2 shows the comparison between the dominant vectors of the depolarization and repolarization loops for the analysis of one subject from the preterm-IUGR and another subject from the preterm-AGA. Furthermore, for the sake of clarity in graphical representation, the projections of the loops on the plane with clearer differences were represented (instead of representing them in the three-dimensional space).

In general, preterm-AGA and preterm-IUGR subjects presented larger values for angle measurement Φ_{R-XY} than controls, being also statistically significant when adjusting the data by age, height, gender and heart rate. In the particular case of preterm-IUGR, the angle difference $\Phi_{R-XY} - \Phi_{T-XY}$ was also significant, being even larger than for the preterm-AGA group. Roundness measurements revealed significant differences between preterm-AGA and control groups, presenting the latter ones lower roundness measurements when analyzing the depolarization loops in the planes XZ and YZ.

4. Discussion of results

This paper reports for the first time significant changes in depolarization-repolarization angles and VCG loop morphology in IUGR and preterm individuals, respectively. These findings support the notion of electrophysiological remodeling in both IUGR and prematurity, and could

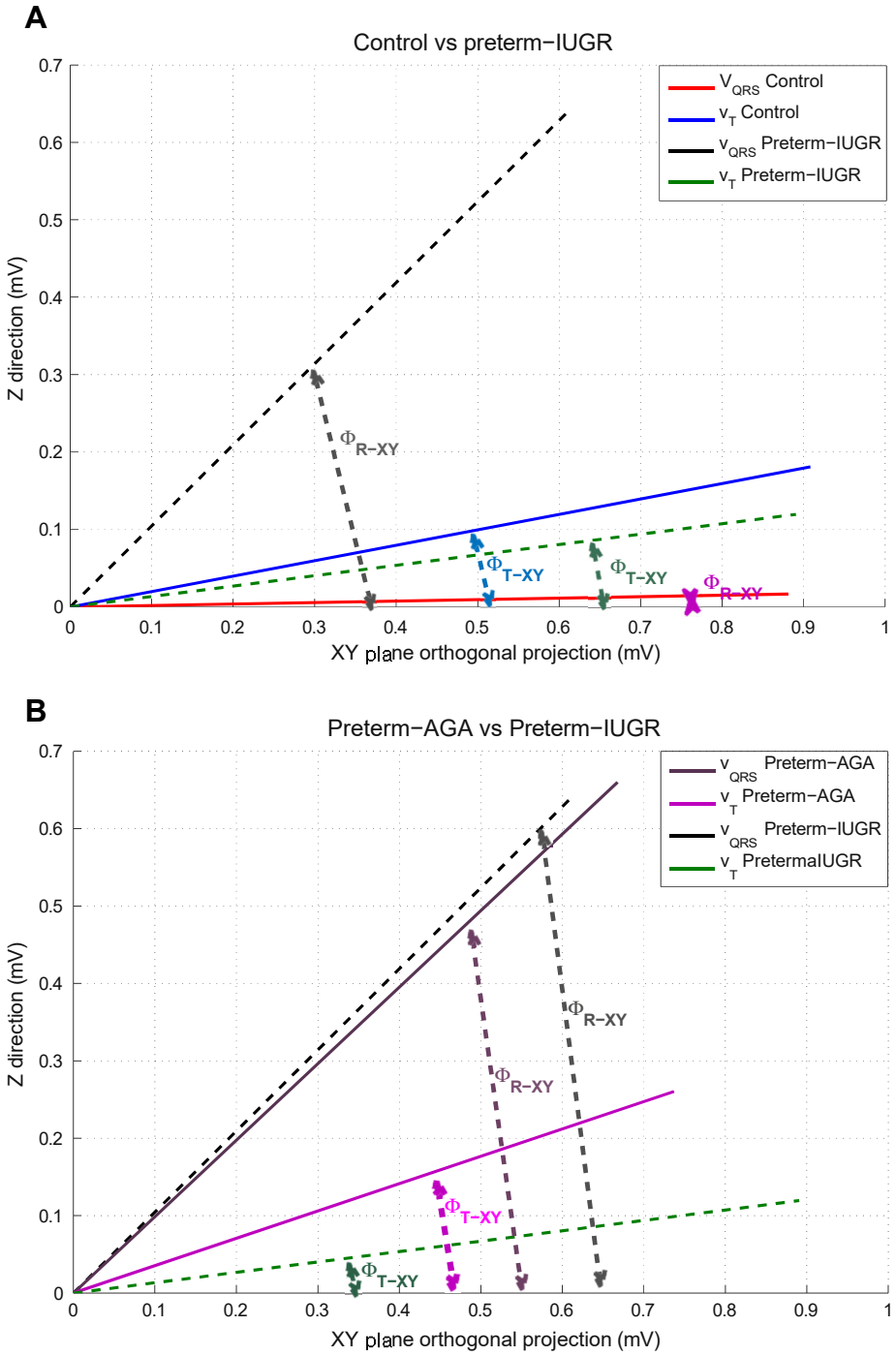

Fig. 2. (A) Projection of dominant vectors of the average depolarization and repolarization loops on XY plane (and the respective absolute angles) for a subject of the control group and a subject from the preterm-IUGR group. (B) Projection of dominant vectors of the average depolarization and repolarization loops on XY plane (and the respective absolute angles) for a subject of the preterm-AGA group and a subject from the preterm-IUGR group.

partially explain the higher cardiovascular morbidity previously reported in these populations.

This study has included a group of preadolescents who suffered severe IUGR in uterus that lead to medically induced preterm delivery. This preterm-IUGR group was characterized by a wider QRS-T angle (θ_{RT}) in relation to body plane, with no significant differences in roundness and planarity. While a non-significant trend to higher values of spatial (θ_{RT}) and frontal ($\theta_{RT\text{-}XY}$) QRS-T angles was observed, significantly higher angles in the frontal plane (XY) could be demonstrated with respect to controls (Table 2). Despite being wider than in controls, their angle values were within the normal limits [16]. Usually, a wider QRS-T angle is derived by changes in T-wave axis, which has been reported to be a risk factor for cardiac events [17,18]. However, in our study wider QRS-T angle in the XY plane was mainly due to changes in QRS axis (although there were also changes in the T-wave -significant for XZ plane, but not significant for XY frontal plane-), suggesting more significant depolarization rather than repolarization abnormalities.

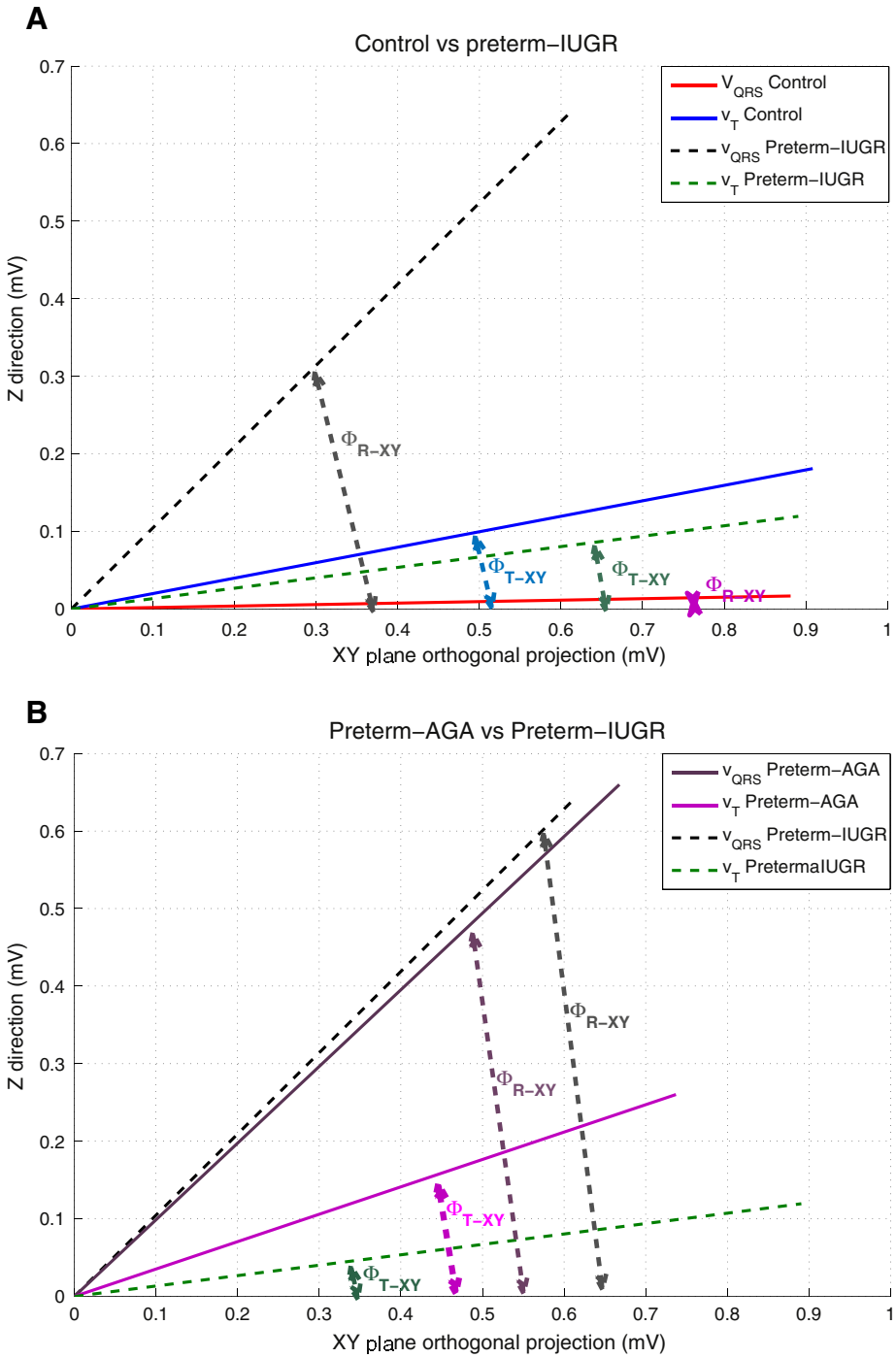

Fig. 2. (A) Projection of dominant vectors of the average depolarization and repolarization loops on XY plane (and the respective absolute angles) for a subject of the control group and a subject from the preterm-IUGR group. (B) Projection of dominant vectors of the average depolarization and repolarization loops on XY plane (and the respective absolute angles) for a subject of the preterm-AGA group and a subject from the preterm-IUGR group.

partially explain the higher cardiovascular morbidity previously reported in these populations.

This study has included a group of preadolescents who suffered severe IUGR in uterus that lead to medically induced preterm delivery. This preterm-IUGR group was characterized by a wider QRS-T angle (θ_{RT}) in relation to body plane, with no significant differences in roundness and planarity. While a non-significant trend to higher values of spatial (θ_{RT}) and frontal ($\theta_{RT\text{-}XY}$) QRS-T angles was observed, significantly higher angles in the frontal plane (XY) could be demonstrated with respect to controls (Table 2). Despite being wider than in controls, their angle values were within the normal limits [16]. Usually, a wider QRS-T angle is derived by changes in T-wave axis, which has been reported to be a risk factor for cardiac events [17,18]. However, in our study wider QRS-T angle in the XY plane was mainly due to changes in QRS axis (although there were also changes in the T-wave -significant for XZ plane, but not significant for XY frontal plane-), suggesting more significant depolarization rather than repolarization abnormalities.